THE INFLUENCE OF pH ON THE STRUCTURE OF TEMPLATED MESOPOROUS SILICAS PREPARED FROM SODIUM METASILICATE

Patricia J. KOOYMAN[a], Markéta SLABOVÁ[b1], Vladimír BOSÁČEK[b2], Jiří ČEJKA[b3], Jiří RATHOUSKÝ[b4,*] and Arnošt ZUKAL[b5]

[a] *National Centre for High Resolution Electron Microscopy, Delft University of Technology, Delft, The Netherlands; e-mail: p.j.kooyman@tnw.tudelft.nl*

[b] *J. Heyrovský Institute of Physical Chemistry, Academy of Sciences of the Czech Republic, Dolejškova 3, 182 23 Prague 8, Czech Republic; e-mail: [1] marketa.slabova@jh-inst.cas.cz, [2] vladimir.bosacek@jh-inst.cas.cz, [3] jiri.cejka@jh-inst.cas.cz, [4] jiri.rathousky@jh-inst.cas.cz, [5] arnost.zukal@jh-inst.cas.cz*

Received February 2, 2001
Accepted March 16, 2001

A recently developed homogeneous precipitation method was used for the investigation of the influence of pH on the structure of mesoporous silicas prepared from sodium metasilicate in the presence of a quaternary alkyl ammonium surfactant as a structure directing agent. The rate of pH decrease affects the assembly of mesoscopically ordered composites and, consequently, the porous structure of mesoporous silicas prepared from them by calcination. Pure MCM-41 molecular sieve was prepared by controlling the pH decrease of the reaction mixture so as to achieve the final pH 7.8. The as-made material prepared at higher pH (final value 10.1) is characterized by a lower degree of silica polycondensation. Due to the shrinkage of this material during calcination, a less well-ordered silica with extraordinary large surface area was prepared. A large decrease in pH (final value 5.2) led to non-organized polycondensation of silica species besides the organized assembly of the ordered material, which resulted in the formation of silica with a bimodal mesoporous structure.

Keywords: Mesoporous silicas; Silicates; Molecular sieves; Homogeneous precipitation; MCM-41; ^{29}Si MAS NMR spectroscopy; Powder X-ray diffraction.

Since the first synthesis of mesoporous molecular sieves[1,2], micelle-templated mesoporous silica has attracted considerable and still growing attention due to the fact that it offers a large surface area (≈1 000 m^2/g) and porous volume (up to ≈2.5 cm^3/g) with a narrow pore size distribution which can be adjusted between 2 and 30 nm. The preparation of this material is based on synergistic self-assembly between silica species and surfactant micelles to form mesoscopically ordered composites[3]. The originally developed mesoporous silicas called MCM-41 and MCM-48 with the hexagonal and cubic structure, respectively, were prepared using quater-

nary alkyl ammonium surfactants. The introduction of anionic[4], neutral[5] and non-ionic[6] surfactants has led to a number of various frameworks of mesoporous silica. Alkyl poly(oxyethylene) and poly(oxyalkylene) block copolymers, such as triblock copolymer poly(ethylene oxide)–poly(propylene oxide)–poly(ethylene oxide), proved to be suitable templates for the synthesis of a large family of highly ordered mesoporous silicas of different structure types[7,8].

At present, different silica sources such as colloidal silica, water-soluble inorganic silicates or esters of orthosilicic acid are used in the syntheses of templated mesoporous silica. Like the synthesis of non-templated porous silica[9], the pH of the reaction mixture plays an important role influencing final structure of the product. In particular the synthesis routes utilizing inorganic silicates are very sensitive to pH. Depending on its value, micelle-templated silicas with different porous structures or morphology features were obtained[10–16].

Recently, a new procedure for the synthesis of mesoporous silica has been developed, which is based on homogeneous precipitation of a solid product from water solution of sodium silicate and a cationic surfactant[17–19]. The uniform acidification of the reaction mixture without local variations in pH is achieved by hydrolysis of appropriate ester of acetic acid. As the pH decrease rate and final pH value can be simply controlled, this synthesis route is suitable for the investigation of the pH influence on the structure of templated silica.

In this work the homogeneous precipitation method was used for the study of the pH influence on the porous structure of mesoporous silicas prepared using sodium metasilicate as a silica source and hexadecyl(trimethyl)ammonium bromide as structure directing agent. The effect of the degree of polycondensation of silica species in the as-made mesoscopically ordered composite on porous structure of the calcined material has been investigated using ^{29}Si MAS NMR spectroscopy.

EXPERIMENTAL

Materials

All the reagents used were obtained from Aldrich: sodium metasilicate (Na_2SiO_3), hexadecyl(trimethyl)ammonium bromide (HDTMABr) and methyl acetate (MeOAc).

Synthesis

The reaction mixture was prepared in a poly(methylpentene) (Nalgene) bottle. In the synthesis, 1.96 g of HDTMABr followed by 2 g of Na_2SiO_3 was dissolved in 1 000 ml of distilled

water, resulting in a clear solution. Afterwards 1.5–5.0 ml of MeOAc was quickly added under vigorous stirring, which was stopped after 30 s. The corresponding molar composition of the reaction mixture was 1 Na_2SiO_3 : 0.33 HDTMABr : 3 390 H_2O : 1.15–3.84 MeOAc.

The reaction mixture, which turned cloudy after 5–10 min after the addition of MeOAc, was aged at ambient temperature for 60 h followed at 90 °C for another 40 h. During the ageing at 90 °C, organic vapour was allowed to evaporate through leaks in the cap of the bottle. The resulting solid product was recovered by filtration, washed with distilled water followed by ethanol, and dried at ambient temperature. The template was removed by calcination at 600 °C (2 °C/min) under flowing air for 20 h.

The samples prepared are listed in Table I.

Instrumentation

^{29}Si MAS NMR spectra were measured at 39.76 MHz on a Bruker DSX200 spectrometer equipped with an MAS probe head using the Hahn echo pulse sequence $\pi/2$–τ–π with proton decoupling. An excitation rf pulse of the Hahn echo pulse sequence was applied with $\pi/2$ pulse 4.5 μs and delay τ = 200 μs in the ^{29}Si channel. Repetition delay from 10 up to 120 s was used. Samples were loaded in 7-mm zirconium oxide rotors spinned at 5 kHz.

Adsorption isotherms of nitrogen at 77 K were taken with a Micromeritics ASAP 2010 instrument. The as-made samples were degassed at ambient temperature for at least 50 h until a pressure of 0.1 Pa was attained; the calcined samples were degassed at 350 °C at the same pressure overnight. Powder X-ray diffraction (XRD) patterns were collected on a Siemens D 5005 diffractometer in the Bragg–Brentano geometry arrangement with CuKα radiation.

Transmission electron microscopy (TEM) was performed using a Philips CM30T electron microscope with a LaB_6 filament as the source of electrons, operated at 300 kV. Samples were mounted on a Quantifoil microgrid carbon polymer supported on a copper grid by placing a few droplets of a suspension of ground sample in ethanol on the grid, followed by drying in ambient conditions.

TABLE I
Preparation of mesoporous silicas using various amounts of methyl acetate

Silica	MeOAc/Na_2SiO_3 (molar ratio)	pH[a]	Q^4/Q^3 [b]
A	1.15	10.1	0.99
B	1.92	7.8	1.22
C	3.84	5.2	1.67

[a] pH was measured after ageing the reaction mixture at 90 °C and subsequent cooling to ambient temperature. [b] Ratio of integral intensities of Q^4 and Q^3 lines.

RESULTS AND DISCUSSION

The initial pH value of the solution of Na_2SiO_3 and HDTMABr used for the synthesis of mesoporous silica was 11.8. The rate of the pH decrease strongly depended on the amount of MeOAc added to this solution. Figure 1 shows the time evolution of pH of the reaction mixtures of samples A, B and C during the aging at ambient temperature. As the hydrolysis of MeOAc is not finished during this aging, the decrease in pH continues in the course of the aging at 90 °C. The final values of the pH are given in Table I.

Nitrogen adsorption isotherms (Fig. 2) demonstrate that the rate of the pH decrease and its final value strongly influence the porous structure of silicas prepared. As all pores in the silica framework of as-made samples A and B are filled with the surfactant micelles, adsorption isotherms of these materials (not shown) are typical of non-porous solids with flat open surface. The isotherm on the calcined sample B exhibits a sudden increase in the adsorption at the relative pressure ≈0.35, which is typical of well-ordered MCM-41 molecular sieves. The adsorption isotherm on the calcined sample A suggests that the pore size of this sample is smaller than that of sample B. The isotherm on calcined sample C shows the presence of a bimodal mesopore structure consisting of smaller MCM-41 mesopores and larger non-MCM-41 ones, which are responsible for the hysteresis loop. In the case of the as-made sample C, the nitrogen isotherm displays a hysteresis loop at relative pressures larger than 0.8, very similar to that ob-

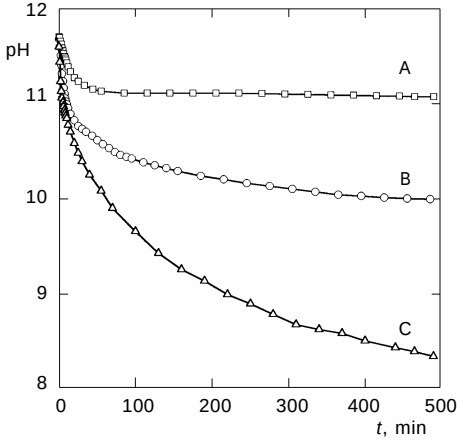

FIG. 1
Time evolution of pH of the reaction mixtures at MeOAc/Na_2SiO_3 molar ratios 1.15 (A), 1.92 (B) and 3.84 (C) during aging at ambient temperature

tained on the calcined sample (Fig. 2). After calcination of this sample the increase in adsorption at relative pressures 0.30–0.35 has appeared as consequence of the surfactant elimination from MCM-41 pores.

The structure parameters of as-made and calcined samples are summarized in Table II. The calcined sample A exhibits an extremely large BET surface area of 1 512 m^2/g. As with this sample the BET equation is valid in the range of relative pressures from 0.06 to 0.11 only, its use cannot be regarded as an appropriate method for the determination of the surface area. The more realistic surface area of sample A was derived using the comparison plot method. In this method the amount adsorbed on the solid under investigation (mmol/g) is plotted against that adsorbed on a non-porous reference silica (mmol/m^2) at the same equilibrium pressure. The slope of the linear part of the comparison plot going through the origin determines the total surface area of the investigated solid[20]. The surface area of 1 235 m^2/g was obtained in this way; it was used for the evaluation of the mean pore diameter of sample A being 2.69 nm. As for the calcined sample B, the pore size of 3.27 nm and volume of 0.719 cm^3/g are typical of the MCM-41 prepared with HDTMABr as the structure directing agent. The sample C is characterized by relatively large volume of the non-MCM-41 mesopores; their mean diameter of 14 nm is identical for both as-made and calcined materials. The non-MCM-41 mesopore surface area and the volume of as-made sample C are smaller than the corresponding parameters of the cal-

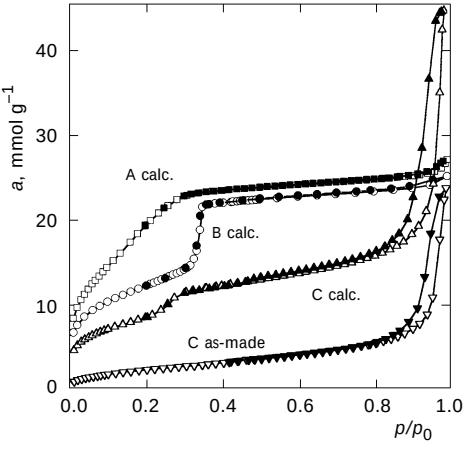

FIG. 2
Adsorption isotherms of nitrogen at 77 K on calcined silicas A and B and as-made and calcined silica C. Solid points denote desorption

cined one, which is an obvious result of the presence of surfactant micelles in the as-made material containing a smaller proportion of silica.

Figures 3 and 4 show the XRD patterns of as-made and calcined samples A and B and calcined sample C. With sample A, the XRD pattern shows some deterioration of structure ordering during calcination. With samples B and C, XRD data confirm a high degree of ordering of sample B and the presence of the MCM-41 structure in sample C. Lattice constants of as-made samples A, B and C, and calcined samples B and C are practically identical ranging from 4.33 to 4.43 nm (Table II). Consequently, the shrinkage of samples B and C during calcination is insignificant. The lattice

TABLE II
Texture parameters of mesoporous silicas

Parameter	Silica					
	A as-made	A calcined	B as-made	B calcined	C as-made	C calcined
a_0, nm	4.43	3.61	4.42	4.35	4.39	4.33
S_{BET}, $m^2\ g^{-1}$	78	1 512	60	976	277	688
S_{CP}, $m^2\ g^{-1}$	–	1 235	–	972	–	658
S_{EXT}, $m^2\ g^{-1}$	78	107	60	94	277	357
S_{MCM-41}, $m^2\ g^{-1}$	–	1 128	–	878	–	301
V_{MCM-41}, $cm^3\ g^{-1}$	–	0.759	–	0.719	–	0.230
D_{MCM-41}, nm	–	2.69	–	3.27	–	3.07
δ_{MCM-41}, nm	–	0.92	–	1.08	–	1.27
$S_{non-MCM-41}$, $m^2\ g^{-1}$	–	–	–	–	231	357
$V_{non-MCM-41}$, $cm^3\ g^{-1}$	–	–	–	–	0.808	1.299
$D_{non-MCM-41}$, nm	–	–	–	–	14	14

a_0, S_{BET}, S_{CP} and S_{EXT} denote respectively the lattice constant, BET surface area, total surface area (determined using the comparison plot method) and the external surface area remaining free after filling up the MCM-41 mesopores. $S_{MCM-41} = S_{CP} - S_{EXT}$, V_{MCM-41}, $D_{MCM-41} = 4\ V_{MCM-41}/S_{MCM-41}$ and δ_{MCM-41} stand for the surface area, volume, pore diameter and pore wall thickness of the MCM-41 structure, respectively. $S_{non-MCM-41}$, $V_{non-MCM-41}$ and $D_{non-MCM-41}$ denote the surface area, volume and mean pore diameter of the system of large mesopores, respectively. Methods for the determination of MCM-41 structure parameters from adsorption and XRD data are given elsewhere[20]. The parameters of the non-MCM-41 mesopore structure were determined from the desorption branch of the hysteresis loop by the Barrett–Joyner–Halenda method[21].

constant of 3.61 nm of calcined sample A reveals its large shrinkage; it is evident that due to this shrinkage sample A is characterized by a worse pore ordering, smaller pore diameter and larger pore wall thickness than sample B (Fig. 3, Table II).

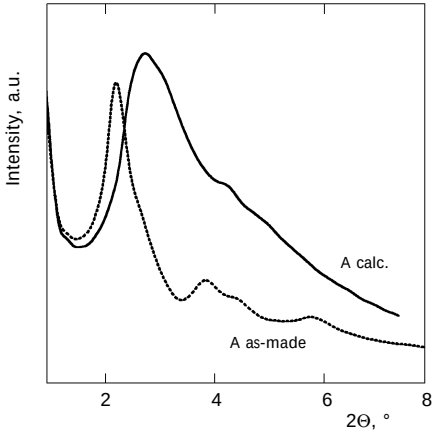

FIG. 3
X-Ray diffractograms of as-made and calcined silica A

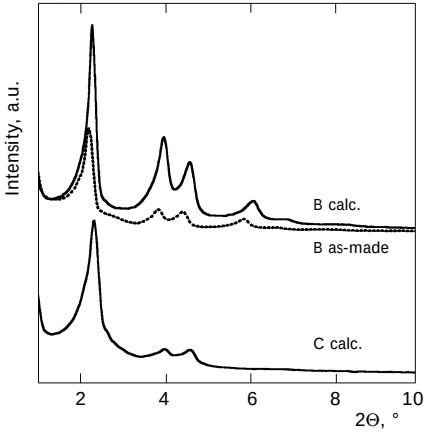

FIG. 4
X-Ray diffractograms of as-made and calcined silica B and calcined silica C

The ^{29}Si MAS NMR spectra of the as-made samples show the degree of silica crosslinking (Fig. 5). The main lines at about –100 and –110 ppm correspond to Q^3 and Q^4 silicate species, respectively. (Q^n species are defined as $Si(OSi)_n(OH)_{4-n}$.) The ratio Q^4/Q^3, which characterizes the degree of silica polycondensation, depends on the final pH value of the reaction mixture (Table I). With sample A, which was prepared in the region of relatively high pH, the Q^4/Q^3 ratio being 0.99 reveals the lowest degree of silica polycondensation. With samples B and C, the Q^4/Q^3 ratio increased to 1.22 and 1.67, respectively, due to a higher degree of silica polycondensation, which is related to the decrease in the final pH of the reaction mixture. Therefore, a large shrinkage of sample A during calcination occurs due to the low degree of silica polycondensation of the as-made material.

Thermogravimetric results confirmed completion of the silica polycondensation of sample A due to calcination. The weight loss of this sample in calcination is 55.2 wt.%. The weight loss of sample B equals 38.6 wt.% only, which is similar to the published values, corresponding to the theoretical content of surfactant[22].

TEM examination of the calcined samples provides structure information, which could not be gained from nitrogen adsorption or X-ray diffraction measurements. The structure of sample A is characterized by the presence of small domains of an ordered mesoporous structure with smaller pore size than that of sample B, which are embedded in the disordered mesoporous

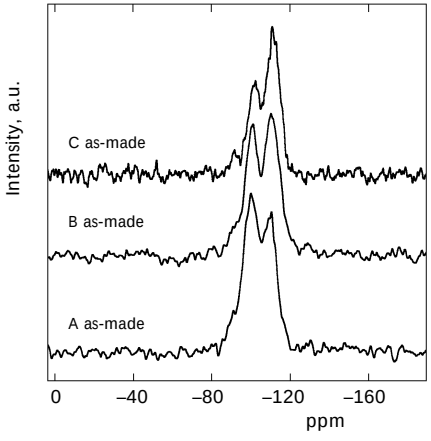

FIG. 5
^{29}Si MAS NMR spectra of as-made silicas A, B and C

material (Fig. 6). Thus the TEM image reveals the character of structure deterioration, which is not apparent from other experimental techniques. The TEM images of sample B (Figs 7 and 8) show a perfect symmetry of pore ordering; no presence of amorphous material or another material with a disordered arrangement of pores was observed. The MCM-41 structure of sample C is viewed side-on with respect to the pores (Fig. 9). The larger mesopores are visible as lighter areas, but their structure is less clear than that of the MCM-41 material. These mesopores are not regularly arranged and do not run through the whole thickness or length of the particle.

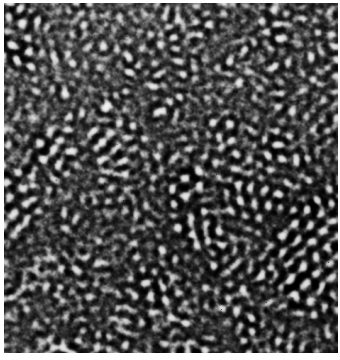

FIG. 6
TEM image (100 nm × 100 nm) of silica A

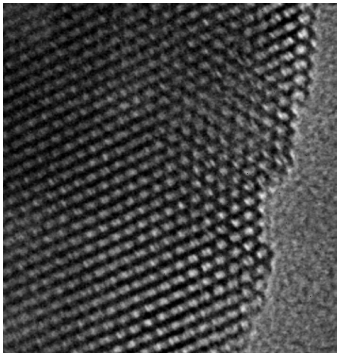

FIG. 7
TEM image (100 nm × 100 nm) of silica B: end-on view of mesopores showing their hexagonal arrangement

A relatively small volume of the MCM-41 mesopores of sample C indicates that only a fraction of silica species was assembled under the organising action of surfactant micelles. As the non-MCM-41 mesopores of as-made sample C are practically empty, they were formed without the controlling action of surfactant micelles because of a too fast and large decrease in pH of the reaction mixture. This conclusion is supported by the TEM examination of sample C because analysis of a number of images of this sample has shown that non-MCM-41 mesopores are mostly present in the particle shell, its core consisting of the MCM-41 structure.

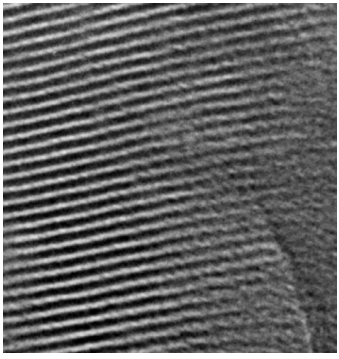

FIG. 8
TEM image (100 nm × 100 nm) of silica B: side-on view with respect to pores

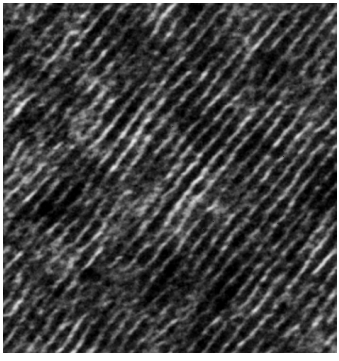

FIG. 9
TEM image (100 nm × 100 nm) of silica C

The conclusions concerning the pore structure of the sample C are also supported by *in situ* investigation of the hexadecyl(trimethyl)ammonium surfactant/silicate system[23], which suggests that the first step in the formation of mesocomposite is the formation of siliceous oligomers. As these oligomers grow, they bind an increasing amount of surfactant ions and, at some point, precipitation of a mesomorphous surfactant ion/polymerized silica complex takes place. If the pH decrease is too fast, the rate of formation of this complex can be smaller than the rate of silica oligomer growth, which causes formation of a non-organized solid phase.

CONCLUSIONS

The rate of the pH decrease during the preparation decisively determines the porous structure of mesoporous silica prepared from sodium metasilicate under the organizing action of quaternary ammonium surfactant micelles. The best-quality siliceous MCM-41 molecular sieve can be prepared by controlling the pH decrease of the reaction mixture so as to reach the final value of 7.8. The as-made material prepared at higher pH is characterized by a lower degree of silica polycondensation. Due to its shrinkage in calcination, a less well-ordered silica with an extraordinary large surface area was prepared. A fast pH decrease causes a partly unorganized polycondensation of silica species, which results in a material with a bimodal mesoporous structure.

P. J. Kooyman acknowledges NWO for financial support. The work of J. Čejka was supported by the Grant Agency of the Academy of Sciences of the Czech Republic (grant No. A4040001). J. Rathouský and A. Zukal are indebted to the Grant Agency of the Czech Republic (grant No. 203/98/1168) for financial support.

REFERENCES

1. Kresge C. T., Leonowicz M. E., Roth W. J., Beck J. S.: *Nature* **1992**, *359*, 710.
2. Beck J. S., Vartuli J. C., Roth W. J., Leonowicz M. E., Kresge C. T., Schmitt K. D., Chu C. T.-W., Olson D. H., Sheppard E. W., McCullen S. B., Higgins J. B., Schlenker J. L.: *J. Am. Chem. Soc.* **1992**, *114*, 10834.
3. Huo Q., Margolese D. I., Ciesla U., Feng P., Gier T. E., Sieger P., Leon P., Petroff P. M., Schüth F., Stucky G. D.: *Nature* **1994**, *368*, 317.
4. Huo Q., Margolese D. I., Ciesla U., Demuth D. G., Feng P., Gier T. E., Sieger P., Firouzi A., Chmelka B. F., Schüth F., Stucky G. D.: *Chem. Mater.* **1994**, *6*, 1176.
5. Tanev P., Pinnavaia T. J.: *Science* **1995**, *267*, 865.
6. Bagshaw S. A., Prouzet E., Pinnavaia T. J.: *Science* **1995**, *269*, 1242.

7. Zhao D., Huo Q., Feng J., Chmelka B. F., Stucky G. D.: *J. Am. Chem. Soc.* **1998**, *120*, 6024.
8. Zhao D., Feng J., Huo Q., Melosh N., Fredrickson G. H., Chmelka B. F., Stucky G. D.: *Science* **1998**, *279*, 548.
9. Iler R. K.: *The Chemistry of Silica*, p. 174. John Wiley, New York 1978.
10. Ryoo R., Kim J. M.: *J. Chem. Soc., Chem. Commun.* **1995**, 711.
11. Lin H.-P., Mou C.-Y.: *Science* **1996**, *273*, 765.
12. Lin H.-P., Cheng S., Mou C.-Y.: *Microporous Mater.* **1997**, *10*, 111.
13. Kruk M., Jaroniec M., Ryoo R., Kim J. M.: *Microporous Mater.* **1997**, *12*, 93.
14. Wang A., Kabe T.: *Chem. Commun.* **1999**, 2067.
15. Sierra L., Guth J.-L.: *Microporous Mesoporous Mater.* **1999**, *27*, 243.
16. Sierra L., Lopez B., Guth J.-L.: *Microporous Mesoporous Mater.* **2000**, *39*, 519.
17. Rathouský J., Zukalová M., Zukal A., Had J.: *Collect. Czech. Chem. Commun.* **1998**, *63*, 1893.
18. Schulz-Ekloff G., Rathouský J., Zukal A.: *Microporous Mesoporous Mater.* **1999**, *27*, 273.
19. Schulz-Ekloff G., Rathouský J., Zukal A.: *J. Inorg. Mater.* **1999**, *1*, 97.
20. Schulz-Ekloff G., Rathouský J., Zukal A. in: *Synthesis of Porous Materials* (M. L. Occelli and H. Kessler, Eds), p. 391. Dekker, New York 1997.
21. Barrett E. P., Joyner L. G., Halenda P. P.: *J. Am. Chem. Soc.* **1951**, *73*, 373.
22. Rathouský J., Zukalová M., Zukal A.: *Collect. Czech. Chem. Commun.* **1998**, *63*, 271.
23. Frasch J., Lebeau B., Soulard M., Patarin J., Zana R.: *Langmuir* **2000**, *16*, 9049.